Molecular dynamics simulation of AFM tip-based hot scratching of nanocrystalline GaAs

Pengfei Fan[1], Saurav Goel[2,3,4*], Xichun Luo[1*], Yongda Yan[5], Yanquan Geng[5], Yang He[5] and Yuzhang Wang[5]

[1] Centre for Precision Manufacturing, DMEM, University of Strathclyde, UK

[2] School of Engineering, London South Bank University, 103 Borough Road, London SE1 0AA, UK

[3] School of Aerospace, Transport and Manufacturing, Cranfield University, Bedfordshire, MK43 0AL, UK

[4] Department of Mechanical Engineering, Shiv Nadar University, Gautam Budh Nagar, 201314, India

[5] Center for Precision Engineering, Harbin Institute of Technology, Harbin, P. R. China

*Corresponding email: goeLs@Lsbu.ac.uk; xichun.luo@strath.ac.uk

Abstract

GaAs is a hard, brittle material and its cutting at room-temperature is rather difficult, so the work explored whether hot conditions improve its cutting performance or not. Atomic force microscope (AFM) tip-based hot machining of the (0 1 0) oriented single crystal GaAs was simulated using molecular dynamics (MD). Three representative temperatures 600 K, 900 K and 1200 K (below the melting temperature of ~1511 K) were used to cut GaAs to benchmark against the cutting performance at 300 K using indicators such as the cutting forces, kinetic coefficient of friction, cutting temperature, shear plane angle, sub-surface damage depth, shear strain in the cutting zone, and stress on the diamond tip. Hotter conditions resulted in the reduction of cutting forces by 25% however, the kinetic coefficient of friction went up by about 8%. While material removal rate was found to increase with the increase of the substrate temperature, it was accompanied by an increase of the sub-surface damage in the substrate. Simulations at 300 K showed four major types of dislocations with Burgers vector 1/2<110>, 1/6<112>, <0-11> and 1/2<1-12> underneath the cutting zone and these were found to cause ductile response in zinc-blende GaAs. Lastly, a phenomenon of chip densification was found to occur during hot cutting which referred to the fact that the amorphous cutting chips obtained from cutting at low temperature will have lower density than the chips obtained from cutting at higher temperatures.

Keywords: AFM Tip-based hot machining; Molecular dynamic (MD) simulation; Single crystal gallium arsenide, Dislocation nucleation

1 Introduction

Gallium arsenide (GaAs) has emerged as a favorable III-V semiconductor compound due to its application in 5G communication devices [1]. GaAs possesses superior physical characteristics such as high-temperature resistance [2], high stopping power [3], high radiation resistance [4], high electronic mobility [5], high magnetic field sensitivity [6] and large band-gap [7]. However, its relatively high nanoindentation hardness (6.9 GPa), elastic modulus (103 GPa) and low fracture toughness (K_{IC}=0.43

MPa $m^{1/2}$) results in poor room-temperature machinability and makes it an even more challenging hard-to-machine material than Si [8][9]. The plasticity index (E/H) of silicon on the (100) orientation is 13.72 while that of GaAs is 14.92 and the brittleness index (H/K_{IC}) of silicon on the (100) orientation is 12.08 in contrast to 16.27 for GaAs. It is well known that the hardness and yield strength of a hard, brittle material decreases at higher temperatures [10] and the fracture toughness increases with the increase of temperature [11]. To this end, nanometric cutting of GaAs substrates at room temperature was recently investigated by the authors [12] and some conceptual fundamental aspects of room-temperature cutting of GaAs and the wear of diamond tool were discussed. In light of previous experience [13], the authors believe that hot machining conditions should improve the machinability of GaAs which became the key objective of this investigation. With the rise of parallel computing and the latest advances in high-performance computing, molecular dynamics (MD) simulation is creating new horizons in the field of materials oriented manufacturing to become a futuristic digital manufacturing tool [14]. A major motivation behind this work is therefore to understand the salient aspects of the AFM tip-based hot machining of GaAs using MD simulations.

In recent years, MD simulation study of hot machining has primarily concentrated on silicon (Si) and silicon carbide (SiC). For example, a comparison study of hot machining of SiC with conventional machining was investigated and it was observed that hot machining reduces the tangential cutting forces and stresses in the cutting zone, however, the shear plane angle stayed invariant. A major concern related to the hot machining is the likelihood of graphitization of the diamond tool which can accelerate tool wear [13]. Moreover, dislocation nucleation and amorphization-based plasticity mechanisms were proposed during hot machining of SiC at temperatures up to 3000 K. A variation in the dislocations behaviour including the formation of multi-junction, Frank-type sessile and stair-rod partials were found when cutting was carried out at temperatures above 900 K [15]. Furthermore, specific cutting energy of SiC showed an increase at cutting temperatures up to 1400 K and a gradual decrease at higher temperatures of 1700 K and 2000 K. Hot nanometric cutting of SiC on different crystal orientations was also investigated. A phenomenon of cleavage was observed in all cases during the cutting of the (111) oriented SiC [16]. During hot machining of Si, the rotational flow of Si underneath the diamond tool similar to the vorticity became more pronounced [17]. Moreover, the depth of sub-surface damage became more pronounced in hot cutting [18], meanwhile the primary shear zone became wider [19]. Furthermore, the few stacking faults were seen to grow during the hot machining of Si [20].

The research so far on GaAs has remained focused on the experimental study of room temperature machining for nanogrooves [21], single-electron transistors [22] or modulation-doped field effect transistors (MODFET) [23] or has explored the origins of ductile-mode machining of GaAs [24] experimentally. To date, there exists no evidence in the literature that clarifies the response of GaAs in hot cutting conditions. An in-depth understanding of nanoscale machining mechanics during hot machining of GaAs continues to remain a knowledge gap. The paper makes use of molecular dynamics (MD) simulation to reveal the influence of heating on the cutting forces, structural changes and stresses in the cutting zone and diamond tip during the AFM tip-based nanomachining of GaAs.

2 MD simulation methodology

The MD simulations were performed on an open source programming code, "Large-scale atomic/molecular massively parallel simulator" LAMMPS [25]. A schematic of the MD simulation model of AFM tip-based nanomachining of GaAs with 1,188,564 atoms (56.9 nm × 22.1 nm × 21.6 nm) is shown in Fig. 1. The diamond tip with 17,132 atoms was treated as a deformable body. The cutting of GaAs was performed on the (0 1 0) surface along the $[\bar{1}\ 0\ 0]$ direction. The atoms within the GaAs workpiece and the diamond tool were assigned three regions, namely boundary region, thermostat region and Newton region. The desired temperature of the Newton atoms (600 K, 900 K, 1200 K and the room temperature 300K) was achieved by equilibrating the sample for about 50 ps by employing a fast and robust Nose-Hoover method [26]. A 3D stress unit region of atoms (1 nm^3) was used to monitor the stress in the cutting zone. Visual molecular dynamics (VMD) [27] and Open Visualization Tool (OVITO) softwares [28] were used to analyse and visualise the simulation results. Further details of the MD simulation model are shown in Table 1.

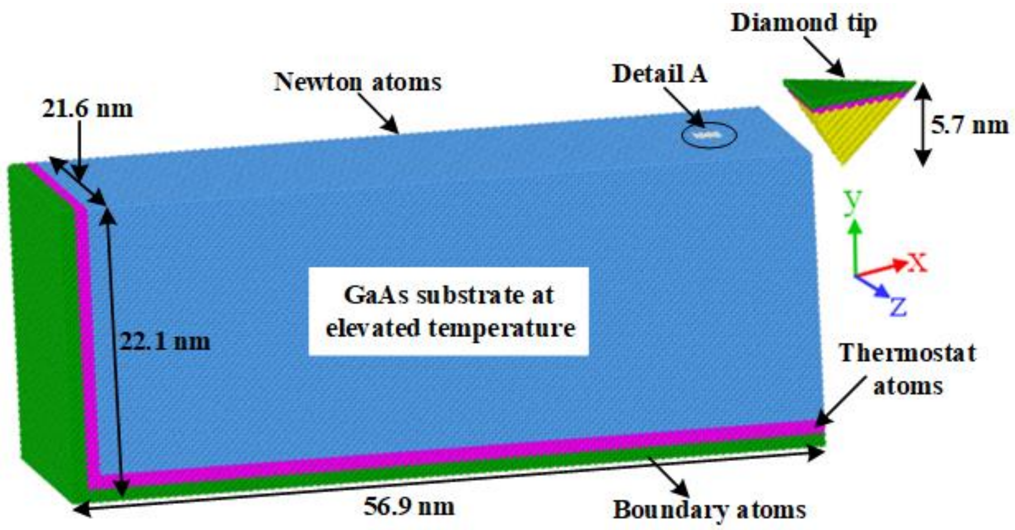

Fig. 1. MD simulation model of AFM tip-based nanomachining of GaAs under pre-heating temperature. Detail A: volume of atoms assigned to monitor stress and temperature during cutting.

Table 1: MD simulation model and cutting condition

Substrate material	Single crystal GaAs
Substrate dimensions	56.9 × 22.1 × 21.6 nm^3 (X, Y and Z direction)
Machining tool	Diamond tip (non-rigid)
GaAs lattice constant	5.65 Å (Zinc blende lattice structure)
Diamond lattice constant	3.56 Å (Diamond cubic lattice structure)
Depth of cut	3 nm
Width of cut	1.7 nm
Cutting distance	10 nm
Cutting velocity of the tool	50 m/s
Crystallographic plane of GaAs substrate and cutting direction	(0 1 0) [$\bar{1}$ 0 0]

Substrate initial temperature before cutting	300 K, 600 K, 900 K, 1200 K
Temperature of the diamond tip	300 K in all MD simulation cases
Boundary conditions	Shrink-wrapped, shrink-wrapped and periodic along the X, Y, and Z directions respectively
Timestep of MD calculation	1 fs

The choice of potential function can make a significant difference on the accuracy of MD results. It is important to choose a robust potential especially when it concerns studying aspects of fracture, wear and plasticity of a material. In this investigation, the cutting of GaAs with a diamond tool required describing the interactions between and among three types of atoms namely, Ga, As and C atoms. Due to the unavailability of a single many-body potential function parameterized to describe all these atoms, a hybrid scheme was employed here using a hybrid/overlay scheme offered by LAMMPS. For the sake of brevity, the details of the potential function (which is readily available from the respective papers [12]) are not repeated here, but generally speaking, the covalently bonded interactions of C-C and the Ga-Ga, As-As and Ga-As interactions were all described by the analytical bond order potential developed by the research group of Albe et al. [29][30]. As for the cross interactions between the atoms of the diamond tool and the Gallium Arsenide workpiece (Ga-C and As-C), a Ziegler-Biersack-Littmark (ZBL) potential function [31] (pair_style zbl in LAMMPS) was used which simply requires the atomic number and cut off parameters as an input. The procedure for calculation of physical stress tensor and ensemble temperature on the group of atoms in the cutting region is well documented in our prior publications and is not repeated for the purpose of brevity [32].

3 Results and discussions

3.1 Cutting forces and temperature

The resultant cutting force was calculated by summing up the component forces between the diamond tip and GaAs substrate in LAMMPS. A comparison of the resultant force variation under four conditions of cutting is shown in Fig. 2 (a). It can be seen that the resultant force (defined as the square sum of two orthogonal forces, normal force and scratching force), experienced a sharp increase at the beginning of the cut until the onset of chip formation (which is referred to as compression dominated regime) and thereafter the force achieved a steady-state. The resultant force was of the order of 100 to 150 nN.

Furthermore, the magnitude of the resultant cutting force during hot machining at 1200 K was 24% lower than that of room temperature nanomachining at 300 K. This noticeable reduction may be attributed to the thermal softening of the workpiece which increases its plasticity index (E/H) and this is consistent with other brittle materials like the single crystal 3C–SiC and silicon [15][16][17][19]. Contrary to a reduction observed in the resultant force, the kinetic coefficient of friction (F_x/F_y) during hot machining went up in comparison to the room temperature machining (see Fig. 2 (b)).

The magnitude of this increase in the value of kinetic coefficient of friction was about 7.83%. Contrary to the previously reported work [33], where a friction drop was reported during hot ploughing until the substrate's melting point, our work revealed an increase in the value of kinetic coefficient of friction which was reported to be the case of only a wearless sliding [34]. During this investigation, the average temperature of the cutting zone in the workpiece was also observed to rise steadily with increasing cutting distance (see Fig. 3). One can see that the local temperature of the cutting zone easily reached a value of above 1000 K during hot machining. Experimentally such a condition has been observed to cause graphitization of diamond [35]. Therefore, the useful life of the diamond tip comes to be in serious jeopardy during hot machining at temperatures close to 1000 K.

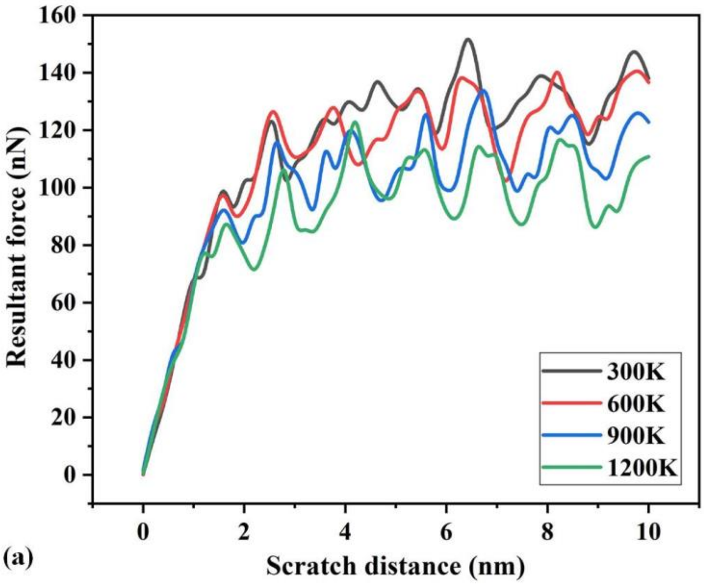

(a)

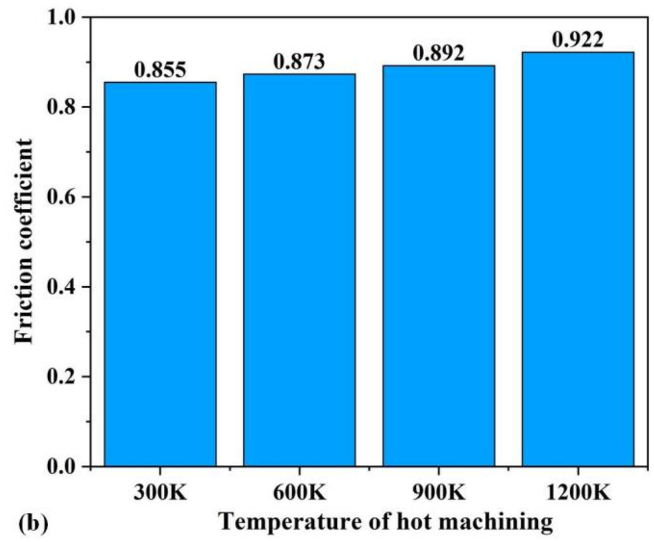

Fig. 2. (a) Variations in the resultant cutting forces with the cutting distance. (b) Variation in the friction coefficient with the cutting temperature.

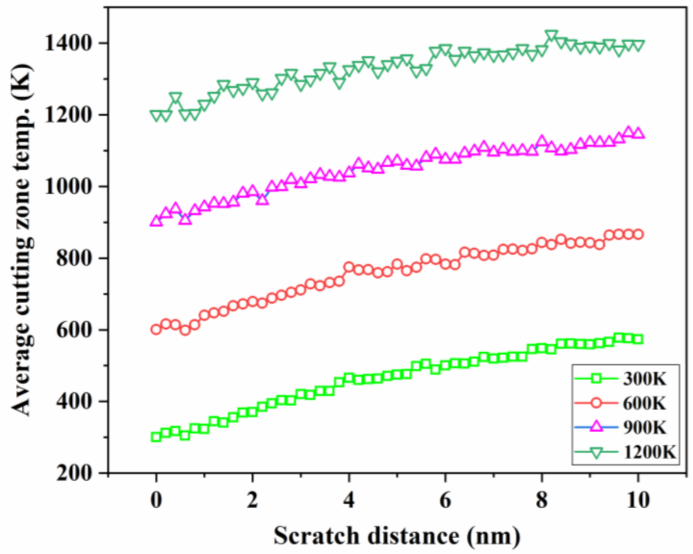

Fig. 3. Variation in the average temperature in the cutting zone of the workpiece under different hot cutting conditions.

3.2 Machining stresses and dislocation nucleation in the cutting zone

It is well known that the Tresca stress and von Mises stress can be used to predict yielding in ductile materials while a Principal stress criterion is more suitable to predict yielding in brittle materials [36]. Single crystal GaAs is hard and brittle at room temperature, but its chips are removed via the ductile-mode so this research looked into the stress tensors and yield criterion that can be applied to describe ductility in GaAs. To achieve this aim, the scalar stress values were obtained in the cutting zone. Here the atomic stress tensor was averaged temporally and then processed using established 3D stress mechanics theory [32], as shown in Fig. 4 (a). It became evident that the magnitude of von Mises stress in the cutting zone was ~6.89 GPa, which appeared close to the experimental nanoindentation hardness [37][38] of GaAs. The result shows that both the von Mises and the minor Principal stress criterion can be used to predict yielding during ductile-mode cutting of GaAs.

Variations of the average hydrostatic stress and von Mises stress at different cutting temperatures are shown in Fig. 4 (b). It shows that the hydrostatic stress and von Mises stress experienced rapid reduction by 60.49% and 58.78% respectively, when cutting temperature increased from 300 K to 1200 K. Temperature dependent reduction in the value of stress in the cutting zone denotes the ease of machinability of GaAs at a higher temperature but below its melting point of 1287°C.

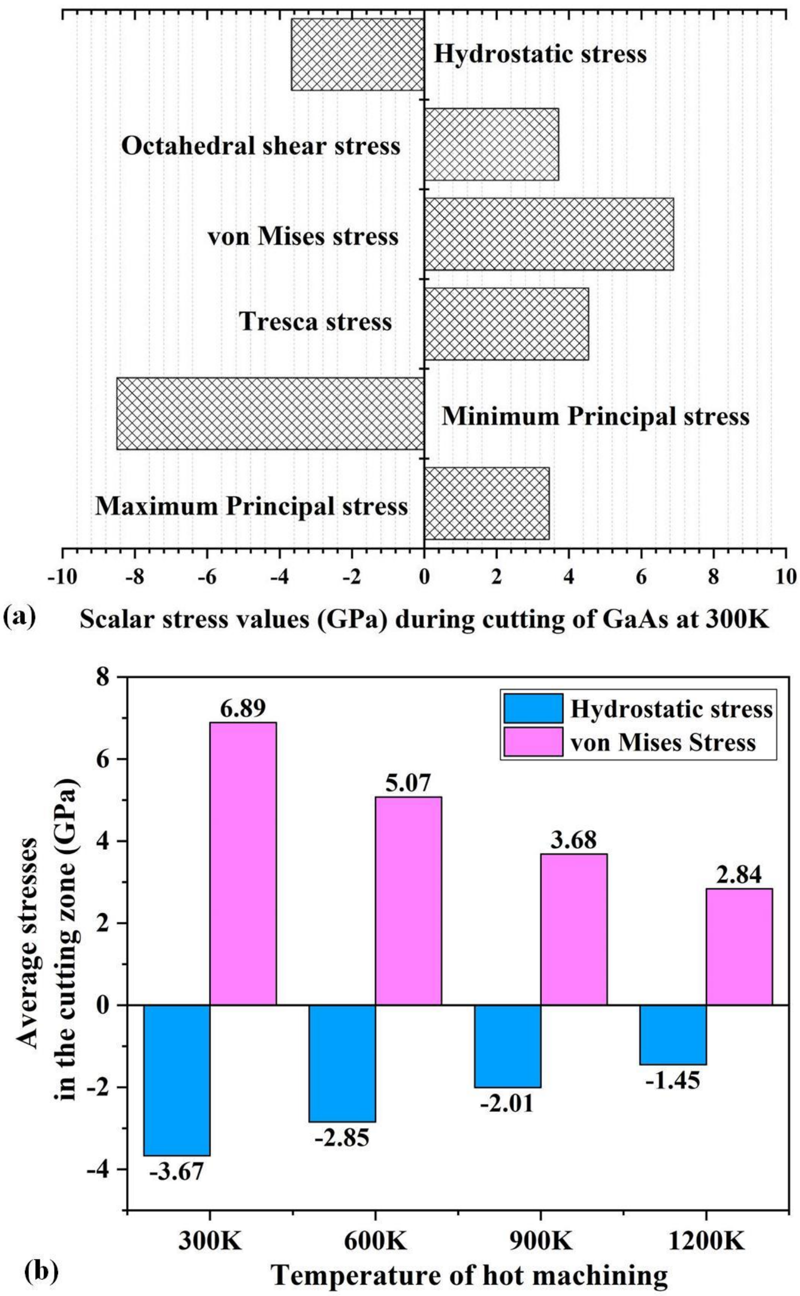

Fig. 4. (a) Scalar stress values (GPa) during cutting of GaAs at 300K. (b) Average value of hydrostatic stress and von Mises stress of the cutting zone at four different temperatures cases.

The research next focuses on understanding the origins of plasticity and hence an automated dislocation extraction algorithm (DXA) [39] was used to detect and identify sub-surface activity in GaAs. Fig. 5 shows the various types of dislocation cloud underneath the machined surface at 300 K. The dislocation extraction algorithm indicated four types of dislocation nucleation with their Burgers vector as 1/2<110>, 1/6<112>, <0-11> and 1/2<1-12>. It can be seen that the predominant dislocation nucleation with the 1/2<110> type dislocation emanates from the primary shear zone of the GaAs substrate. It was also observed that the 1/2<110> type dislocation dissociated into Shockley partials, 1/6<121> (30°) and 1/6<211> types (60°) dislocations interconnected by an intrinsic stacking fault (ISF). This phenomenon of dislocation dissociation has commonly been observed in silicon under moderately applied stress and temperature conditions [40] and it shows level of similarities in the way zinc-blende structure yields akin to a diamond lattice structure. Beside two other dislocations of type <0-11> and 1/2<1-12> were also seen present in the cutting zone.

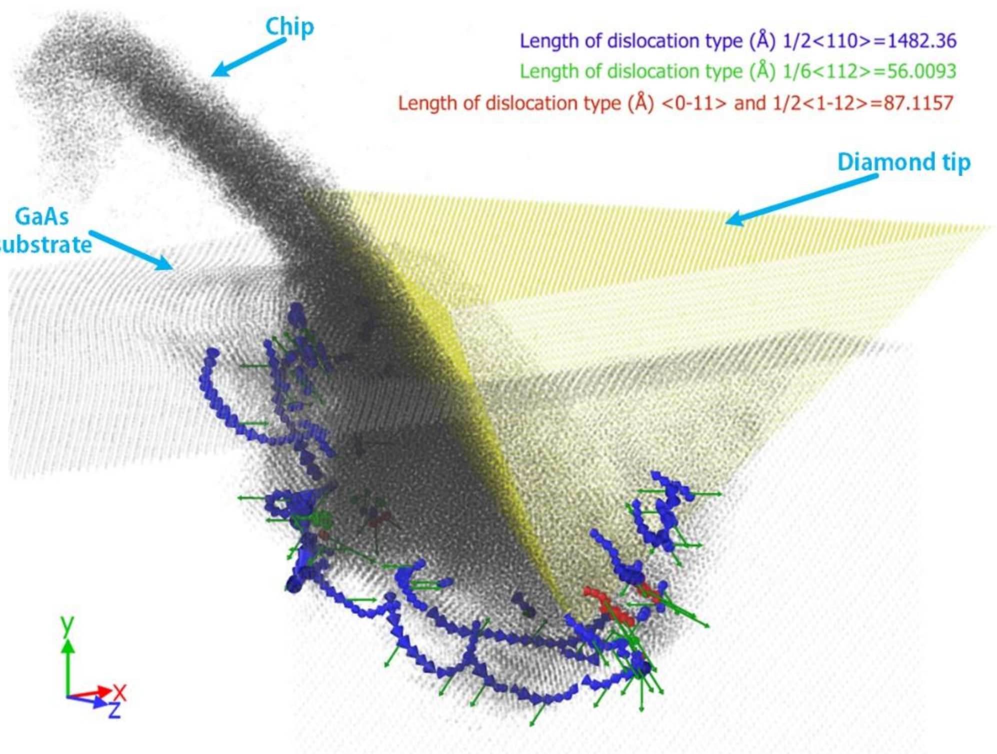

Fig. 5. Dislocation nucleation during scratching of GaAs at 300 K at a cutting distance of 10 nm.

Next the research used atomic-level strain tensors before cutting (initial configuration) to compare the strain after cutting 10 nm (deformed configuration) GaAs [41][42]. The local atomic shear strain i.e. von Mises strain has been reported to describe well the local inelastic deformation [19][43]. The Green-Lagrangian strain tensor matrix η_i was derived from the local deformation gradient tensor matrix J_i and the initial gradient tensor matrix I (see Eq. (1)).

The local atomic shear strain was computed by Eq. (2), in which η_{ij} represents the six gradient tensor components, and its distributions in two representative cases during cutting at 300K and at 1200K are shown in Fig. 6.

$$\eta_i = \frac{1}{2}(J_i J_i^T - I) \quad (1)$$

$$\eta_i^{Mises} = \sqrt{\eta_{yz}^2 + \eta_{xz}^2 + \eta_{xy}^2 + \frac{(\eta_{yy}^2 - \eta_{zz}^2) + (\eta_{xx}^2 - \eta_{zz}^2) + (\eta_{xx}^2 - \eta_{yy}^2)}{6}} \quad (2)$$

It was observed that shear strain accumulates in the primary shear zone where the workpiece atoms experienced inelastic deformation and the magnitude of this strain decreases with the cutting temperature due to fact that the deformation is partially assisted by the thermal energy.

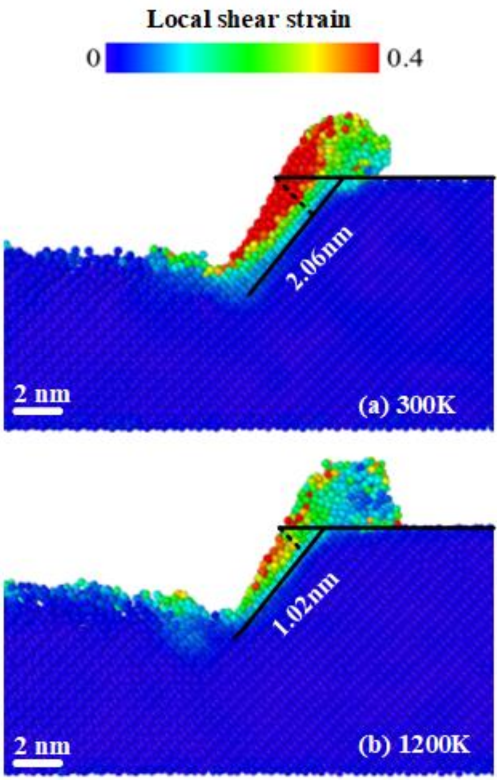

Fig. 6. The local shear strain distribution of the cutting zone at 300 K and 1200 K, respectively.

3.3 Stresses in the diamond tip

Figure 7 shows the variation in the stresses experienced by the diamond tip during cutting of GaAs during various cutting conditions. The magnitude of the hydrostatic stress and von Mises stress were seen to be of the order of 6 GPa and 9 GPa, respectively, which was approximately one fifth and one twentieth of that during cutting of silicon [44] and silicon carbide [11], respectively. Also, the magnitude of stress on the tool reduces by around 20% while comparing the cutting from 300 K to 1200 K which speaks for lower cutting resistance of the workpiece during hot cutting.

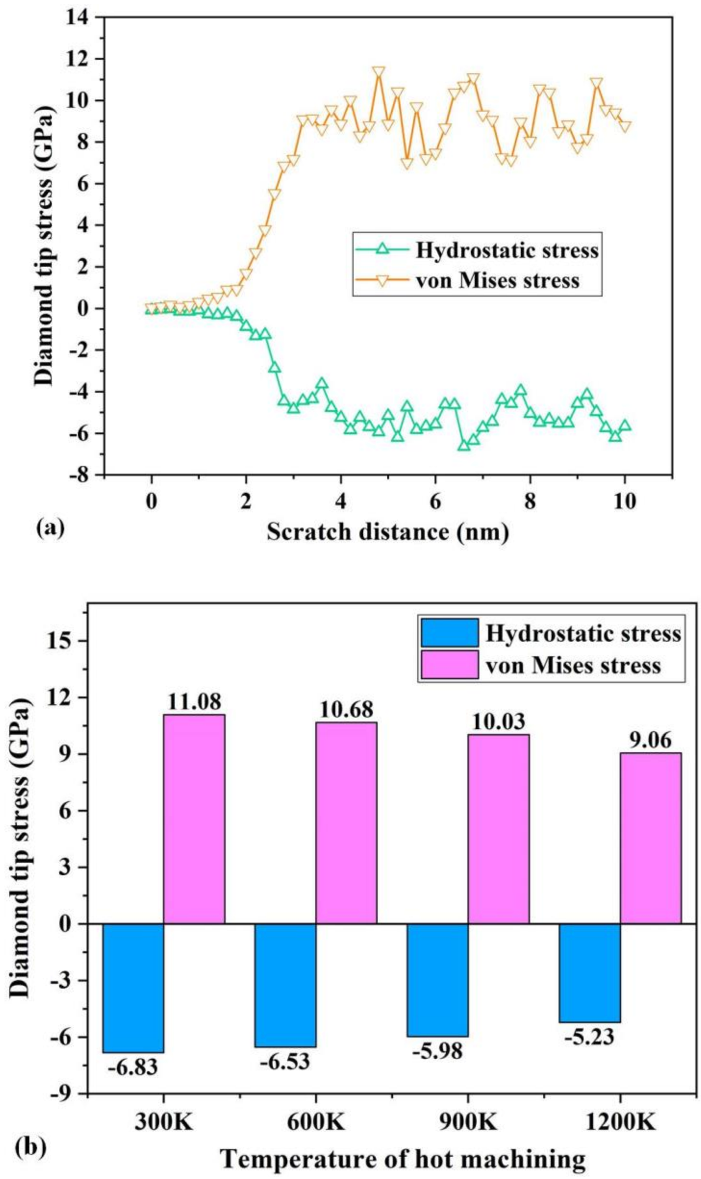

Fig. 7. (a) Variations in the stress experienced by the diamond tip during cutting at 300K and (b) Average value of hydrostatic stress and von Mises stress in the diamond tip at four different temperatures.

3.4 Shear plane angle and sub-surface damage

The shear plane angle (as shown in Fig. 8) represents the position of the primary shear zone relative to the horizontal plane and it was used to describe the machinability of the GaAs workpiece [13]. The shear plane angle was calculated by Eq. (3).

$$\tan\theta = \frac{r\cos\alpha}{1-r\sin\alpha} \quad (3)$$

where θ and α refers to the shear plane angle and rake angle of the diamond tip, respectively. The r is the chip ratio between uncut chip thickness and cut chip thickness. It was found that the shear plane angle reduced by approximately 4.33 degrees when cutting at 1200 K compared to 300 K. Further details may be seen from Table 2. The reduction of shear plane angle during hot machining suggests that the tangential cutting forces (F_x) become dominant over normal forces (F_y), which explains an improved cutting action and improved machinability of GaAs at high temperature.

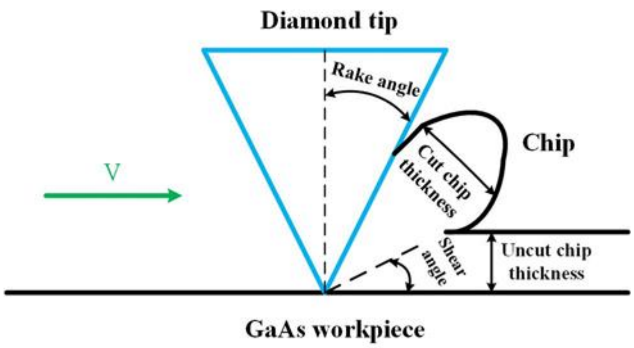

Fig. 8. Schematic diagram of chip formation during AFM tip-based nanomachining of GaAs process.

Table 2: The comparison of shear plane angle for four different temperature cases.

Cases	Nanoscratching temperature	Ratio of uncut chip thickness to cut chip thickness (r)	Shear plane angle (θ)
1	300K	0.456	27.16 deg
2	600K	0.441	26.15 deg

3	900K	0.418	24.70 deg
4	1200K	0.389	22.83 deg

The research finally examines the extent of sub-surface damage at various cutting temperatures and these results are shown in figure 9. It can be seen from Fig. 9 (a)(b) that the depth of sub-surface damage in the machined surfaces increases with the increase of machining temperature, this is one of the drawbacks of hot machining. One of the reasons for seeing larger sub-surface damage is that hot cutting can weaken the interatomic bonding strength resulting in easier damage penetration and more widespread influence of even a low stress value [16]. This behavior was also observed during the cutting of silicon [18] and silicon carbide [16]. Furthermore, as shown in Fig. 9 (c), the number of atoms in the cutting chip grew with the hotness of the workpiece and it suggests that the hot cutting chips are denser than the chips cut at lower temperature.

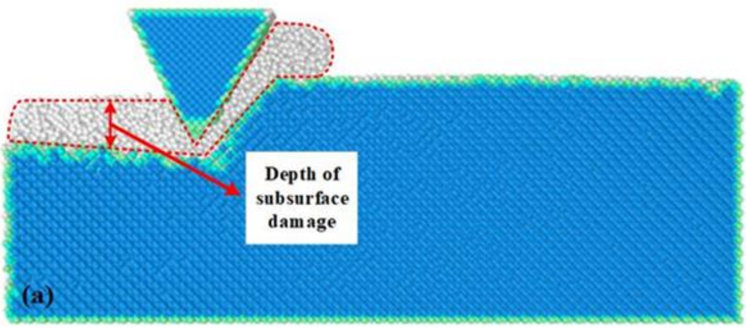

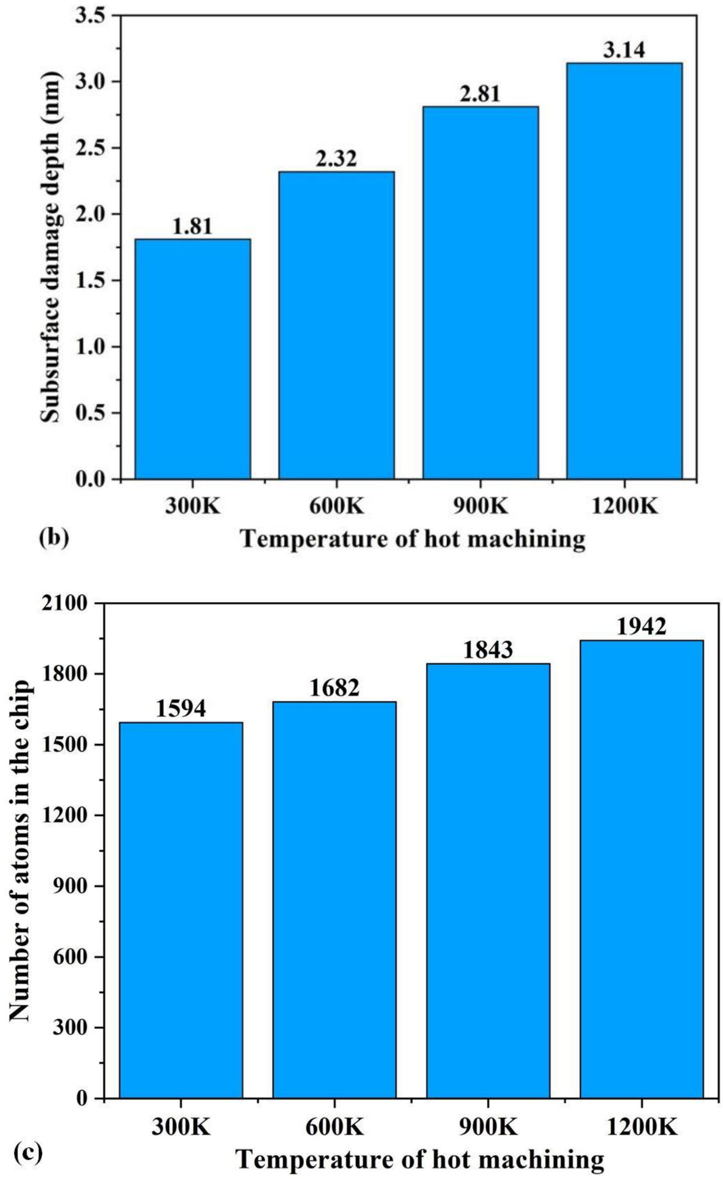

Fig. 9. (a) Schematic diagram of the depth of sub-surface damage. (b) Variation in the sub-surface damage depth at different temperatures. (c) Evolution of the number of atoms in the cutting chips.

4. Conclusions

This work investigated the AFM tip-based hot cutting of single crystal GaAs and benchmarked the cutting performance at room temperature. The investigation made use of molecular dynamics simulations to reveal several new aspects about the hot machining as summarized below:

1. It was found that while hot machining causes material's thermal softening which improves material's machinability evident from lower cutting stresses and cutting forces, the kinetic coefficient of friction between the tool and the workpiece increases with temperature which is in sharp contrast to the published literature.
2. Four major types of dislocations including perfect dislocations and Shockley partials were observed to bring ductility in GaAs during its cutting. The dislocations extracted from the simulation had Burgers Vectors as 1/2<110>, 1/6<112>, <0-11> and 1/2<1-12> respectively.
3. It was surprisingly observed that the hot machining condition leads to an increased extent of sub-surface damage and there is also a trade-off with the use of cutting temperature as graphitization of diamond (even at low cutting stresses) can trigger by virtue of cutting temperature.
4. A new observation of chip densification is being reported for the first time i.e. the cutting chips obtained after machining at higher temperature were found to have more atoms than the chips obtained at lower cutting temperature and it showed a possibility of high density amorphization at higher cutting temperature.

Acknowledgement

The authors would like to thank EPSRC (EP/K018345/1 and EP/T024844/1) and the Royal Society-NSFC international exchange programme (IEC\NSFC\181474) to provide financial support to this research.

SG is particularly thankful to the Research support provided by the UKRI via Grants No. EP/L016567/1, EP/S013652/1, EP/T001100/1, EP/S036180/1 and EP/T024607/1. Additionally, the support received from H2020 (Cost Actions (CA18125, CA18224, CA17136 and CA16235), Royal Academy of Engineering via Grants No. IAPP18-19\295, TSP1332 and EXPP2021\1\277 and Newton Fellowship award from the Royal Society (NIF\R1\191571) is also acknowledged. SG also accessed the Isambard Bristol, UK supercomputing service via Resource Allocation Panel (RAP) as well as ARCHER2 resources (Project e648). The authors also acknowledge the use of the EPSRC (EP/K000586/1) funded ARCHIE-WeSt High-Performance Computer at the University of Strathclyde.

Data statement

All data underpinning this publication are openly available from the University of Strathclyde Knowledge Base at http://10.15129/6fd249b4-861f-4f7b-a34f-ad336205fa64.

Conflict of Interest: The authors declare that they have no conflict of interest.

References

[1] H. J. Ahn, W. Il Chang, S. M. Kim, B. J. Park, J. M. Yook, and Y. S. Eo, "28 GHz GaAs pHEMT MMICs and RF front-end module for 5G communication

systems," *Microw. Opt. Technol. Lett.*, vol. 61, no. 4, pp. 878–882, 2019.

[2] H. Altuntas and S. Ozcelik, "The interface states and series resistance analyzing of Au/SiO 2/n-GaAs at high temperatures," *J. Alloys Compd.*, vol. 577, pp. 143–147, 2013.

[3] N. Sathish, I. Kyriakou, D. Emfietzoglou, and A. P. Pathak, "Stopping power of GaAs for swift protons: Dielectric function and optical-data model calculations," *Nucl. Instruments Methods Phys. Res. Sect. B Beam Interact. with Mater. Atoms*, vol. 268, no. 11–12, pp. 1723–1726, 2010.

[4] S. Kawakita *et al.*, "High efficiency and radiation resistant InGaP/GaAs//CIGS stacked solar cells for space applications," *Conf. Rec. IEEE Photovolt. Spec. Conf.*, vol. 2016-Novem, pp. 2574–2577, 2016.

[5] Y. Song, X. Zhang, X. Yan, Q. Liao, Z. Wang, and Y. Zhang, "An enzymatic biosensor based on three-dimensional ZnO nanotetrapods spatial net modified AlGaAs/GaAs high electron mobility transistors," *Appl. Phys. Lett.*, vol. 105, no. 21, 2014.

[6] J. Jadczak, M. Kubisa, K. Ryczko, L. Bryja, and M. Potemski, "High magnetic field spin splitting of excitons in asymmetric GaAs quantum wells," *Phys. Rev. B - Condens. Matter Mater. Phys.*, vol. 86, no. 24, 2012.

[7] F. Martelli, G. Priante, and S. Rubini, "Photoluminescence of GaAs nanowires at an energy larger than the zincblende band-gap: Dependence on growth parameters," *Semicond. Sci. Technol.*, vol. 30, no. 5, pp. 1–6, 2015.

[8] F. Ericson, S. Johansson, and J.-Å. Schweitz, "Hardness and fracture toughness

of semiconducting materials studied by indentation and erosion techniques," *Mater. Sci. Eng. A,* vol. 105–106, no. Part 1, pp. 131–141, 1988.

[9] H. Huang, B. R. Lawn, R. F. Cook, and D. B. Marshall, "Critique of materials-based models of ductile machining in brittle solids," *J. Am. Ceram. Soc.*, vol. 103, no. 11, pp. 6096–6100, 2020.

[10] N. Huang, Y. Yan, P. Zhou, R. Kang, D. Guo, and S. Goel, "Elastic recovery of monocrystalline silicon during ultra-fine rotational grinding," *Precis. Eng.,* vol. 65, no. February, pp. 64–71, 2020.

[11] S. Z. Chavoshi, "An investigation on the mechanics of nanometric cutting for hard- brittle materials at elevated temperatures," University of Strathclyde, 2016.

[12] P. Fan, S. Goel, X. Luo, Y. Yan, Y. Geng, and Y. Wang, "An atomistic investigation on the wear of diamond during atomic force microscope tip-based nanomachining of gallium arsenide," *Comput. Mater. Sci.*, vol. 187, no. October 2020, p. 110115, 2021.

[13] S. Goel, W. Bin Rashid, X. Luo, A. Agrawal, and V. K. Jain, "A Theoretical Assessment of Surface Defect Machining and Hot Machining of Nanocrystalline Silicon Carbide," *J. Manuf. Sci. Eng.*, vol. 136, no. 2, p. 021015, 2014.

[14] S. Goel *et al.*, "Horizons of modern molecular dynamics simulation in digitalized solid freeform fabrication with advanced materials," *Mater. Today Chem.*, vol. 18, p. 100356, 2020.

[15] S. Z. Chavoshi and X. Luo, "Molecular dynamics simulation study of deformation mechanisms in 3C-SiC during nanometric cutting at elevated temperatures," *Mater. Sci. Eng. A*, vol. 654, pp. 400–417, 2016.

[16] S. Z. Chavoshi and X. Luo, "Atomic-scale characterization of occurring phenomena during hot nanometric cutting of single crystal 3C-SiC," *RSC Adv.*, vol. 6, no. 75, pp. 71409–71424, 2016.

[17] S. Z. Chavoshi, S. Goel, and X. Luo, "Molecular dynamics simulation investigation on the plastic flow behaviour of silicon during nanometric cutting," *Model. Simul. Mater. Sci. Eng.*, vol. 24, no. 1, 2015.

[18] S. Z. Chavoshi and X. Luo, "An atomistic simulation investigation on chip related phenomena in nanometric cutting of single crystal silicon at elevated temperatures," *Comput. Mater. Sci.*, vol. 113, pp. 1–10, 2016.

[19] S. Z. Chavoshi, S. Goel, and X. Luo, "Influence of temperature on the anisotropic cutting behaviour of single crystal silicon: A molecular dynamics simulation investigation," *J. Manuf. Process.*, vol. 23, pp. 201–210, Aug. 2016.

[20] S. Z. Chavoshi, S. Xu, and X. Luo, "Dislocation-mediated plasticity in silicon during nanometric cutting: A molecular dynamics simulation study," *Mater. Sci. Semicond. Process.*, vol. 51, pp. 60–70, 2016.

[21] C. K. Hyon, S. C. Choi, S. W. Hwang, D. Ahn, Y. Kim, and E. K. Kim, "Direct nanometer-scale patterning by the cantilever oscillation of an atomic force microscope," *Appl. Phys. Lett.*, vol. 75, no. 2, pp. 292–294, 1999.

[22] H. W. Schumacher, U. F. Keyser, U. Zeitler, R. J. Haug, and K. Eberl,

"Controlled mechanical AFM machining of two-dimensional electron systems: Fabrication of a single-electron transistor," *Phys. E Low-Dimensional Syst. Nanostructures*, vol. 6, no. 1, pp. 860–863, 2000.

[23] M. Versen, B. Klehn, U. Kunze, D. Reuter, and A. D. Wieck, "Nanoscale devices fabricated by direct machining of GaAs with an atomic force microscope," *Ultramicroscopy*, vol. 82, no. 1–4, pp. 159–163, 2000.

[24] J. Chen, X. Luo, F. Ding, X. Rao, and J. Zhang, "Fundamental study of diamond turning of single crystal gallium arsenide," *Precis. Eng.*, vol. 62, pp. 71–82, 2020.

[25] S. J. Plimpton, "Fast parallel algorithms for short range molecular dynamics," *J. Comput. Phys.*, vol. 117, pp. 1–19, 1995.

[26] S. Nose, "A unified formulation of the constant temperature molecular-dynamics methods," *J. Chem. Phys.*, vol. 81, pp. 511–519, 1984.

[27] W. Humphrey, A. Dalke, and K. Schulten, "VMD - Visual Molecular Dynamics," *J. Mol. Graph.*, vol. 14, pp. 33–38, 1996.

[28] A. Stukowski, "Visualization and analysis of atomistic simulation data with OVITO-the Open Visualization Tool," *Model. Simul. Mater. Sci. Eng.*, vol. 18, no. 1, 2010.

[29] D. A. Murdick, X. W. Zhou, H. N. G. Wadley, D. Nguyen-Manh, R. Drautz, and D. G. Pettifor, "Analytic bond-order potential for the gallium arsenide system," *Phys. Rev. B - Condens. Matter Mater. Phys.*, vol. 73, no. 4, pp. 1–20, 2006.

[30] D. K. Ward, X. W. Zhou, B. M. Wong, F. P. Doty, and J. A. Zimmerman, “Analytical bond-order potential for the cadmium telluride binary system,” *Phys. Rev. B - Condens. Matter Mater. Phys.*, vol. 85, no. 11, pp. 1–19, 2012.

[31] J. F. Ziegler, M. D. Ziegler, and J. P. Biersack, “SRIM - The stopping and range of ions in matter (2010),” *Nucl. Instruments Methods Phys. Res. Sect. B Beam Interact. with Mater. Atoms*, vol. 268, no. 11–12, pp. 1818–1823, 2010.

[32] S. Goel, A. Kovalchenko, A. Stukowski, and G. Cross, “Influence of microstructure on the cutting behaviour of silicon,” *Acta Mater.*, vol. 105, pp. 464–478, 2016.

[33] D. Ceresoli and E. Tosatti, “Peak Effect versus Skating in High Temperature Nanofriction,” *Nat. Mater.*, vol. 6, no. 3, pp. 230–234, 2007.

[34] S. Goel, A. Stukowski, G. Goel, X. Luo, and R. L. Reuben, “Nanotribology at high temperatures,” *Beilstein J. Nanotechnol.*, pp. 586–588, 2012.

[35] N. S. Xu, J. Chen, and S. Z. Deng, “Effect of heat treatment on the properties of nano-diamond under oxygen and argon ambient,” *Diam. Relat. Mater.*, vol. 11, no. 2, pp. 249–256, 2002.

[36] G. E. Dieter, “Mechanical Metallurgy,” *McGraw-Hill B. Co., New York*, 1986.

[37] L. Xu, L. Kong, H. Zhao, S. Wang, S. Liu, and L. Qian, “Mechanical behavior of undoped n-type GaAs under the indentation of berkovich and flat-tip indenters,” *Materials (Basel).*, vol. 12, no. 7, pp. 1–10, 2019.

[38] T. H. Fang, W. J. Chang, and C. M. Lin, “Nanoindentation and nanoscratch characteristics of Si and GaAs,” *Microelectron. Eng.*, vol. 77, no. 3–4, pp. 389–

398, 2005.

[39] A. Stukowski, V. V. Bulatov, and A. Arsenlis, "Automated identification and indexing of dislocations in crystal interfaces," *Model. Simul. Mater. Sci. Eng.*, vol. 20, no. 8, 2012.

[40] M. Ganchenkova and R. M. Nieminen, *Mechanical Properties of Silicon Microstructures*. Elsevier Inc., 2015.

[41] F. Shimizu, S. Ogata, and J. Li, "Theory of shear banding in metallic glasses and molecular dynamics calculations," *Mater. Trans.*, vol. 48, no. 11, pp. 2923–2927, 2007.

[42] M. L. Falk and J. S. Langer, "Dynamics of viscoplastic deformation in amorphous solids," *Phys. Rev. E*, vol. 57, no. 6, p. 14, 1998.

[43] S. Goel, N. H. Faisal, V. Ratia, A. Agrawal, and A. Stukowski, "Atomistic investigation on the structure-property relationship during thermal spray nanoparticle impact," *Comput. Mater. Sci.*, vol. 84, pp. 163–174, 2014.

[44] S. Goel, "An atomistic investigation on the nanometric cutting mechanism of hard, brittle materials," Heriot-Watt University, 2013.